Full length article

# Improved fatigue resistance of gradient nanograined Cu

Jianzhou Long [a, 1], Qingsong Pan [a, 1], Nairong Tao [a], Ming Dao [b], Subra Suresh [c, *], Lei Lu [a, **]

[a] Shenyang National Laboratory for Materials Science, Institute of Metal Research, Chinese Academy of Sciences, Shenyang, 110016, People's Republic of China
[b] Department of Materials Science and Engineering, Massachusetts Institute of Technology, Cambridge, MA, 02139, USA
[c] Nanyang Technological University, Singapore, 639798, Republic of Singapore

## ARTICLE INFO

## ABSTRACT

Cyclic stresses generally lead to fatigue damage and failure with important implications for material and component design, safety, performance and lifetime costs in major structural applications. Here we present unique results for copper to demonstrate that a thin superficial layer of graded surface nanostructure over a coarse-grained core suppresses strain localization and surface roughening, thereby imparting unprecedented resistance to both low-cycle and high-cycle fatigue without compromising ductility. Progressive homogenization of the surface-graded copper is shown to be superior in fatigue properties compared to that of any of its homogeneous counterparts with micro-, submicro- or nano-grained structures. Since the findings here for enhancing resistance to fatigue are broadly applicable to a wide spectrum of engineering metals and alloys, the present results offer unique pathways to mitigate fatigue damage using a broad variety of processing routes, geometric design considerations, and structural parameters in many practical applications.

## 1. Introduction

Developing strategies to protect materials against fatigue damage and failure is of importance in many engineering applications from the perspectives of scientific research, material design, performance of components, and lifetime cost savings [1]. The imposition of fluctuating mechanical loads on homogeneous crystalline metals and alloys leads to a continuous change in microstructure with increasing fatigue cycles [1,2]. This change is reflected in progressive accumulation of defects and their reorganization into internal microstructures such as dislocation dipoles and cells, persistent slip bands, and low-angle grain boundaries during different stages of fatigue [2–4]. Even in initially atomically-smooth-surfaced metals and alloys, the significant roughening of surfaces that accompanies cyclic deformation and damage can lead to the formation of intrusions and extrusions [2,5,6]. These surface sites serve as micro-notches where fatigue cracks nucleate and advance into the interior during cyclic loading to eventually cause catastrophic failure [1,6,7].

In homogenous metals, refinement of grain size from micro-crystalline or coarse-grained (CG, with average grain size typically greater than 1 μm) to sub-microcrystalline or ultra-fine-grained (UFG, with an average grain size in the range of 100 nm to several hundred nm) and nano-grained (NG, with average grain size below 100 nm) scales generally results in an effective increase in strength by suppressing dislocation activities [8]. Both enhanced resistance to fatigue crack initiation and higher fatigue endurance limit develop in UFG and NG metals during stress-controlled high-cycle fatigue [9–12]. However, grain size refinement in a structural alloy also leads to substantial reduction in ductility [8,13], almost without exception, along with deterioration in crack-propagation resistance at low-amplitude cyclic stresses, and exacerbates failure in strain-controlled low-cycle fatigue [8–11]. Correspondingly, uniform grain size reduction also causes shortened low-cycle fatigue life and pronounced cyclic softening in UFG and NG alloys [14,15]. These undesirable consequences of fatigue arise from microstructural instability and cyclic-deformation-induced local damage accumulation, such as that produced by shear banding and/or abnormal grain coarsening [11,15–17]. These processes, in turn, severely limit the practical utility of grain-refinement strategies for homogeneous high-strength alloys in fatigue-critical applications [8,11,12].

Controlled introduction of engineered two-dimensional internal

* Corresponding author.
** Corresponding author.
 *E-mail addresses:* ssuresh@ntu.edu.sg (S. Suresh), llu@imr.ac.cn (L. Lu).
[1] Contributed equally.

interfaces at nanoscale, such as nanoscale twin boundaries, could offer a pathway for substantial strengthening while preserving acceptable levels of ductility, fracture toughness and fatigue resistance [18—22]. However, for structural engineering components with complex shapes and large dimensions, it is currently not feasible to produce such initially coherent and stable nano-twin structures of homogeneous alloys in sufficient sizes and quantities required for large engineering components [23].

Materials in which spatial gradients in structural features are purposely introduced from the surface to the interior are, in some cases, known to exhibit superior mechanical characteristics compared to their homogenous counterparts of appropriately comparable composition [24—26]. Specifically, certain spatial gradients introduced in composition in glass-infiltrated alumina and silicon nitride, which promote controlled variations in elastic properties as a function of depth beneath a surface, can lead to substantial improvements in resistance to indentation damage and cracking [24,27,28]. These elastic spatial gradients beneath surfaces are also known to suppress damage and cracking during frictional contact sliding [29]. The introduction of plasticity gradients produced by spatial variation in grain size, while preserving elastic homogeneity, was also found to enhance "ductility" during normal indentation [25]. Here gradients in grain size, from a nano-grained Ni—W surface to larger grains in the interior, were shown to increase pile-up around indentation that was greater than that achievable in any of the homogeneous counterparts. Several surface treatment procedures have been developed to introduce surface gradient structure; examples include: ball burnishing [30], laser shock peening [31], surface mechanical attrition treatment [32], and sliding deformation techniques [33,34]. Building on these observations, studies have also shown how surface gradients involving nanostructures could impart, or at least preserve, ductility in strong UFG and NG metals [35—38]. It was shown that the high-cycle fatigue endurance limit of a variety of metals can be markedly improved via gradient nanostructures with the presence of compressive residual stress [31,39—41]. However, application of such strategies to improve fatigue damage tolerance and failure resistance in both high-cycle and low-cycle regimes has thus far remained unexplored.

Here we present a unique experimental study of the effect of controlled introduction of a relatively thin superficial layer of nanograins on structure evolution, strength, ductility, hardness, high-cycle endurance limit as well as total fatigue life under strain-controlled low-cycle fatigue in pure CG copper at room temperature. We demonstrate that cyclic mechanical loading causes progressive homogenization of grain size through the cross-section. This change in microstructure effectively suppresses both strain localization and surface roughening concurrently, thereby enabling unprecedented resistance to both low-cycle and high-cycle fatigue without compromising ductility. These mechanistic origins of improvements to fatigue resistance are applicable to a wide variety of metals and alloys suitable for a diverse range of engineering structures used in air, ground and marine transportation, civil engineering infrastructure, and consumer products. Hence the results of this study offer novel and unique pathways and a broad framework for designing and tailoring the structural features of engineering metals through controlled introduction of gradients in grain size through a variety of processing routes.

## 2. Methods

### 2.1. Materials

Commercial purity copper rods (99.97 wt%) consisting of equiaxed coarse grains (with an average grain size of 21 μm after annealing at 723 K for 1 h) were first machined into dog-bone shaped cylindrical specimens with a gauge diameter of 6 mm and a gauge length of 12 mm (Inset in Fig. 1f). Then, both the gauge section and arc transitions of these CG Cu specimens were subjected to surface mechanical grinding treatment (SMGT) at cryogenic temperature (~173 K) to produce a nanograined (GNG) surface layer (hereafter referred to as GNG/CG Cu) [35]. During SMGT process, the Cu rod was rotated at a velocity of 600 rpm and a hemi-spherical WC/Co tool tip (with a radius of 3 mm) penetrated into the rod surface over a depth of 40 μm with a sliding velocity of 20 mm/min. For each specimen, the SMGT process was repeated eight times with a total penetration depth of about 320 μm, in order to achieve thick NG and UFG layers. After SMGT process, the surface of GNG/CG Cu rod was found to be smooth with a surface roughness (Ra, defined as arithmetical mean deviation of the assessed surface profile) of 300 nm and no cracks were detected.

In some of the experiments, the NG surface layer of the GNG/CG Cu specimens was removed via mechanical milling so as to produce specimens, labelled as (GUFG/CG) Cu, which only had an UFG layer as the surface layer for comparison tests.

### 2.2. Uniaxial tensile tests

Uniaxial tensile tests of the GNG/CG, GUFG/CG and CG Cu specimens were performed on an Instron 5982 servohydraulic testing machine (Instron Corporation, Canton, MA, USA) at a strain rate of 0.1% s$^{-1}$. An Instron static axial clip-on extensometer with a gauge length of 10 mm was used to calibrate and measure the strain upon loading. To obtain each data set, at least three repeat tensile tests of each test sample were performed.

### 2.3. Tension-compression fatigue tests

Uniaxial symmetric tension-compression cyclic tests of GNG/CG, GUFG/CG and CG Cu specimens were performed on an Instron 8874 servohydraulic testing machine under constant stress- and strain-control at room temperature in air. Before cyclic deformation, the specimens were electrochemically polished to obtain a smooth surface with negligible surface roughness (with a root-mean-square surface asperity roughness value, $R_a < 170$ nm) to establish a reference case for subsequent observation of surface fatigue morphologies. Under strain control, a dynamic strain gauge extensometer with a gauge length of 10 mm was clamped on the specimen surface for accurate measurement and closed-loop control of cyclic strain amplitude. The strain resolution was better than 0.01%. A triangular waveform loading profile with a cyclic strain rate of 0.2% s$^{-1}$ was used. The imposed total strain amplitudes ($\Delta\varepsilon_t/2$) were 0.29% and 0.50%, which lie in the typical strain amplitude ranges (~0.1%—~0.50%) for the standard strain-controlled low-cycle fatigue tests for single-crystal Cu, CG-Cu and UFG-Cu [1,5,11]. Each strain-controlled cyclic test was stopped when the resultant stress amplitude decreased by 50% relative to the reference stress amplitude at 50$^{th}$ cycles. In addition, a set of GNG/CG Cu specimens were cyclically deformed at $\Delta\varepsilon_t/2 = 0.5\%$, but interrupted at different preset cycles (namely $N = 4\%$, 20% and 40%$N_f$) and then fully unloaded. Under stress control, a sinusoidal waveform with a frequency of 30 Hz was used. The imposed stress amplitudes ($\Delta\sigma/2$) ranged from 78 to 140 MPa for GNG/CG Cu and from 56 to 140 MPa for CG Cu. To obtain each data set, at least three repeat cyclic loading tests of each case were performed at each $\Delta\sigma/2$ or $\Delta\varepsilon_t/2$.

### 2.4. Microstructure observation

The cross-sectional microstructures of GNG/CG, GUFG/CG and CG Cu before and after cyclic deformation were characterized by using the FEI Nova Nano 430 scanning electron microscope (SEM,
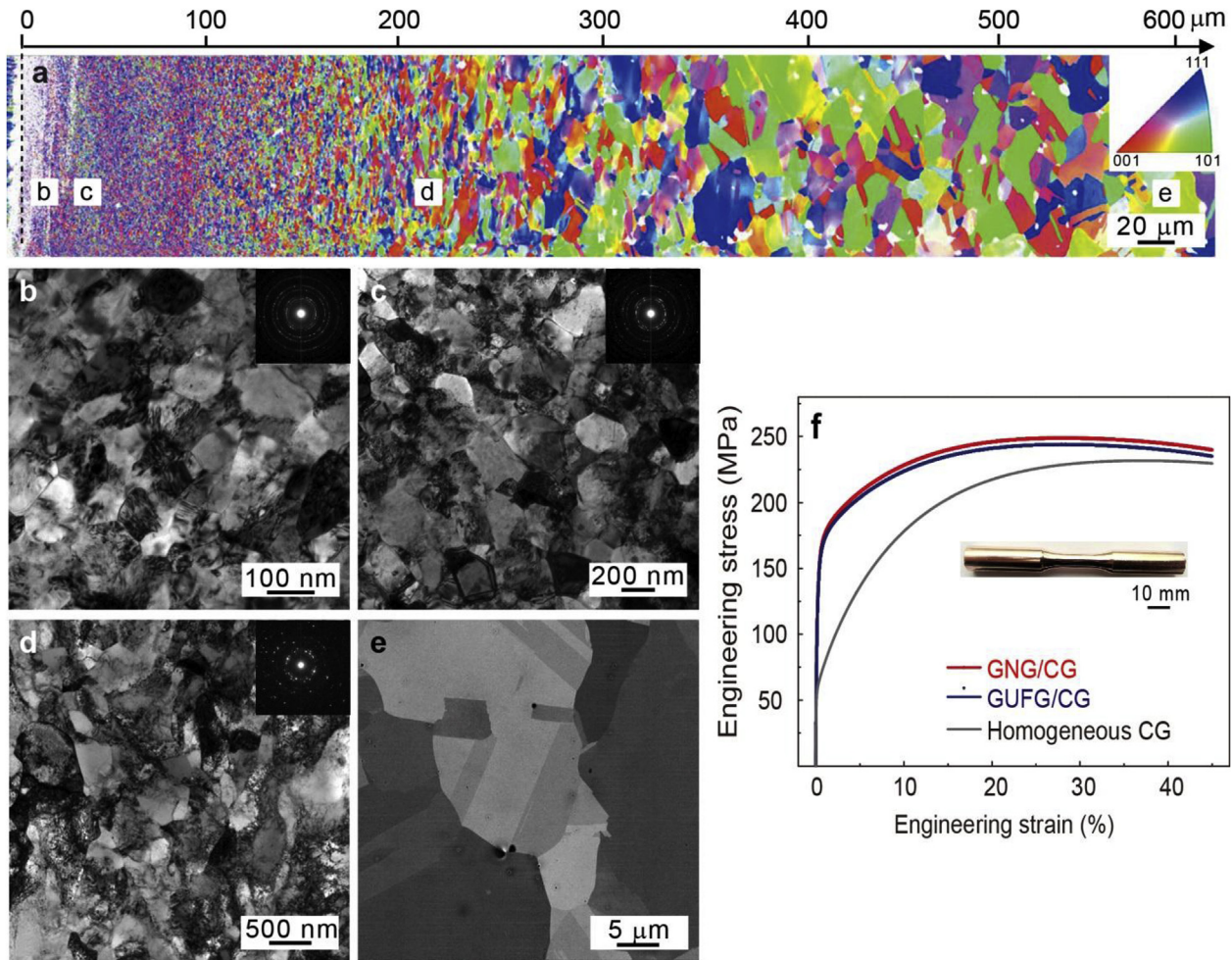
**Fig. 1. Graded surface nanostructure and its tensile properties. a**, Cross-sectional EBSD image of GNG/CG Cu produced via surface mechanical grinding treatment. The corresponding higher-magnification bright-field TEM and SEM images in regions marked "b", "c", "d" and "e" in Fig. 1a are shown in **b-e**, respectively. Top surface of the sample is outlined by a dashed line in **a**. Insets in **b-d** show selected area electron diffraction patterns (SAED). **f**, Engineering stress versus engineering strain curves of GNG/CG, GUFG/CG and homogeneous CG Cu samples. The inset is an image of GNG/CG Cu specimen before tensile test.

FEI, Hillsbora, Oregon, USA) and FEI Tecnai F20G2 transmission electron microscope (TEM, FEI, Hillsbora, Oregon, USA) Electron backscatter diffraction (EBSD) analysis of GNG/CG Cu was carried out under a voltage of 20 kV and a current of 6.0 nA with a step size of 20 nm. The misorientation angles between grains were determined by EBSD analysis. A pure Cu layer was first electro-deposited onto the treated surface of the GNG/CG and GUFG/CG samples. Then, the cross-sectional SEM and TEM foils were cut parallel to the cyclic loading axis by an electrical spark machine, and were subsequently mechanically polished and electro-polished. The TEM Cu foils were finally thinned by twin-jet polishing in an electrolyte of phosphoric acid (25%), alcohol (25%) and deionized water (50%) at about $-10\,°C$. The average size of grains or cells was determined from TEM images by utilizing the linear intercept method. At least 500 grains or cells at each depth of GNG/CG were measured to obtain the average value.

Three-dimensional surface features of GNG/CG, GUFG/CG and CG Cu after cyclic deformation were investigated by using Olympus LEXT OLS4000 confocal laser scanning microscope (CLSM, Olympus, Shibuya, Tokyo, Japan) with a height resolution of 10 nm.

### 2.5. Microhardness tests

Microhardness tests were carried out on cyclically deformed

GNG/CG Cu by using a Mitutoyo MVK-H3 microhardness tester (Mitutoyo L.m.t., Takashita, Tokyo, Japan) with a load of 5 g and a holding time of 10 s. The microhardness value at each depth of GNG/CG samples was obtained by averaging at least 10 measurements, while the error bar is the mean±standard deviation (SD).

## 3. Results

### 3.1. Microstructure and tensile properties

A well-controlled spatial gradation in grain size from the surface to the interior (Fig. 1a) was introduced in CG Cu cylinders with a diameter of 6 mm by recourse to surface mechanical grinding treatment, SMGT (see Methods). Roughly equiaxed nano-sized grains are formed in the outermost 20 μm-thick layer (the region marked "b" in Fig. 1a, comprising the NG layer) which has an average grain size of 60 nm (Fig. 1b). The grains gradually increase in size to the UFG structure with a grain size of 100 nm to 1 μm over a depth of 20–220 μm beneath the surface (the region marked "c" in Fig. 1a), as shown in more detail in Fig. 1c. Here both the NG and UFG layers with a total depth of 220 μm below the free surface are collectively referred to as the gradient nanograined (GNG) layer. Most grains in GNG layer are separated by curved high-angle grain boundaries (GBs) (Fig. 1b–c) and contain a high density of

dislocations (Fig. 1b and c), consistent with the structure typically found in plastically deformed metals [8]. Beneath the GNG layer, at 220—600 μm below the surface, marked "d" in Fig. 1a, exists a deformed CG layer. This layer is characterized by dislocation tangles and/or cells with sizes ranging from sub-μm to μm (Fig. 1d). Beyond a depth of 600 μm from the surface, in the region marked "e" in Fig. 1a, over a distance that spans several tens of mm in gauge length (inset in Fig. 1f), the specimen comprises a CG core populated by crystals with average grain size of 21 ± 5 μm and relatively free of dislocations prior to the fatigue test (Fig. 1e). This heterogeneous core structure with a GNG surface layer and CG core is hereafter referred to as GNG/CG Cu.

Monotonic tensile test of GNG/CG Cu showed its superior tensile properties: (0.2% offset) yield strength of 142 ± 7 MPa, twice that of homogeneous CG, and uniform tensile strain of 29.5 ± 1.6%, comparable to its homogenous CG counterpart (Fig. 1f).

### 3.2. Fatigue behaviors

We conducted both stress-controlled and strain-controlled uniaxial symmetric tension-compression fatigue tests on GNG/CG and homogenous CG Cu over a wide range of stress and strain amplitudes, respectively. The stress amplitude versus fatigue life curve (or $S-N$ curve) in Fig. 2a reveals that the resistance of the graded GNG/CG Cu to stress-controlled high-cycle fatigue is superior to that of homogeneous CG and UFG counterparts. All open symbols denote experimental results reported to date on fatigue life of UFG Cu [14—17]. The large scatter band seen here for UFG arises from different methods employed to produce nanostructures

through severe plastic deformation. The fatigue endurance limit, which represents fully-reversed cyclic stresses under which the total fatigue life of GNG/CG Cu lasts at least $10^7$ cycles, is as high as 98 MPa (Fig. 2a). This is almost twice that of homogeneous CG (56 MPa) and nearly comparable or smaller than that achievable in homogeneous UFG counterparts [14—17,42,43]. Surface-graded GNG/CG Cu is able to achieve this high fatigue strength while maintaining its tensile strength and strain at levels comparable to that of ductile CG Cu. Fig. 2b shows the normalized stress amplitude by the ultimate tensile strength $\sigma_{UTS}$ plotted against the number of stress reversals $2N_f$ to failure. It is found that the fatigue ratio, defined as the ratio of endurance limit at $10^7$ cycles to $\sigma_{UTS}$, is 0.4 for GNG/CG, which is also about twice that for homogenous CG and for most of UFG Cu reported in the literature [14—17,42,43].

In distinct contrast to the cyclic hardening of CG metals [3,44] and cyclic softening of UFG metals [14—16] under strain control, cyclic stability at constant stress amplitude essentially begins to occur in GNG/CG Cu after a short initial hardening stage that lasts only about 20 fatigue cycles (Fig. 2b). At a given total strain amplitude ($\Delta\varepsilon_t/2$), the stress amplitude ($\Delta\sigma/2$) that the GNG/CG Cu is capable of sustaining is much higher than that of CG Cu. Surprisingly, the low-cycle fatigue lifetime of GNG/CG is about twice that of CG Cu which, owing to its good ductility, also displays the longest strain-controlled low-cycle fatigue life among the three homogeneous structures: CG, UFG and NG [1,8,11]. These results indicate that introducing gradient surface nanostructures on a CG core can effectively enhance low-cycle fatigue resistance, with a total low-cycle fatigue life that is even better than that achieved by any of its homogeneous constituent structures [3,11,24]. The
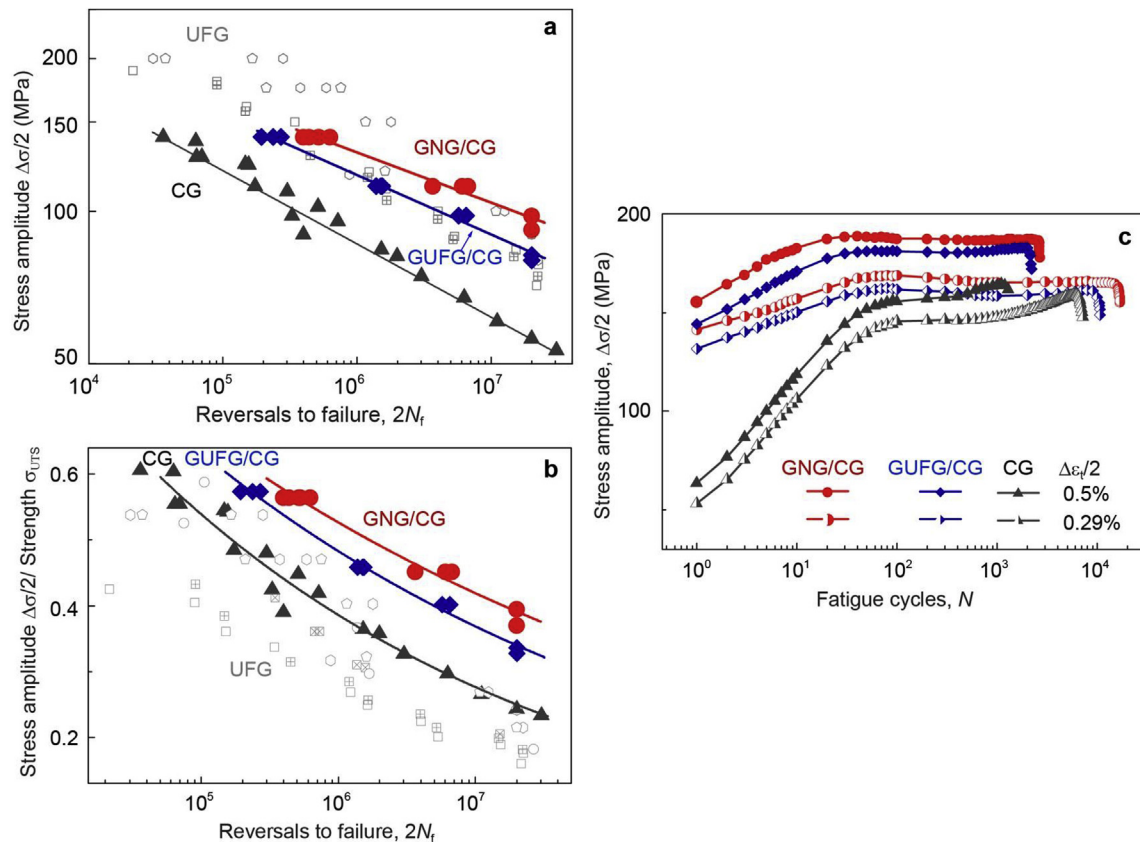


**Fig. 2.** Fatigue properties of GNG/CG , GUFG/CG and homogeneous CG Cu samples. Dependence of the high-cycle fatigue life ($N_f$) on the stress amplitude ($\Delta\sigma/2$) (**a**) and on the stress amplitude ($\Delta\sigma/2$)/tensile strength ($\sigma_{UTS}$) under stress control (**b**), respectively. **c**, Cyclic stress response ($\Delta\sigma/2$) at total strain amplitude ($\Delta\varepsilon_t/2$) of 0.29% and 0.5%, respectively. For comparison, $\Delta\varepsilon_t/2$- $N$ and/or $\Delta\sigma/2$ versus $Nf$ data of homogeneous CG- and UFG- Cu14-17,21 are also included.

foregoing results thus provide the surprising, but clear demonstration that superior all-around fatigue properties, with a concurrent improvement in both low-cycle fatigue life and high-cycle failure endurance limit, can be achieved in surface-graded GNG/CG Cu as compared to homogeneous structures involving either CG or UFG Cu.

### 3.3. Fatigue-induced microstructure homogenization

In order to elucidate the mechanisms of enhanced fatigue resistance arising from the introduction of a thin GNG surface layer on CG core, we examine its structural changes induced by the cyclic loading. For this purpose, we choose GNG/CG Cu subjected to a constant total cyclic strain amplitude, $\Delta\varepsilon_t/2 = 0.5\%$, as a typical example. Cross-sectional observation of fatigued GNG/CG using electron backscatter diffraction (EBSD) reveals in Fig. 3a that the spatial distribution of grain size in the as-fabricated GNG layer, seen in Fig. 1a prior to the fatigue test, completely disappears due to cyclic straining. Cyclic loading leads to continuous coarsening of the graded surface layer until it is replaced by a nearly homogenous grain structure (left part of Fig. 3a), while there is no visible change in grain size in CG core under SEM and EBSD observations. The top GNG surface layer here now comprises roughly equiaxed grains, approximately 1 μm in diameter (Fig. 3b and c). Most grains are

clean with negligible intra-crystalline dislocations, and they are separated by sharp high-angle GBs (Fig. 3b, c and 4b). Pole figures in Fig. 4d show that no strong texture can be detected for micro-size grains in fatigued GNG layer, analogous to that in the as-SMGT state (Fig. 4c). These results indicate that these grains in GNG layer are randomly oriented, consistent with the trends revealed by selected area electron diffraction (SAED) patterns (inset in Fig. 3b and c).

By contrast, higher resolution TEM observation indicates that well-developed dislocation cells in low-angle misorientation (generally less than 2° and hardly detectable via EBSD) are formed in deformed CG and CG core layers after cyclic deformation (Fig. 3d and e). Fig. 5 shows TEM observations of microstructures of CG core after different cycles. A high density of randomly distributed dislocations is detected in the CG core fatigued at $\Delta\varepsilon_t/2$ of 0.5% after 4% of fatigue life cycle ($N_f$), as shown in Fig. 5a. With increasing fatigue cycles, we observe accumulation and typical arrangement of dislocations which results in the formation of dislocation cells at $N = N_f$ (Fig. 5b). Such a cyclic behavior of the CG core in GNG structure is identical to that observed in the homogeneous CG during cyclic loading [2,4]. The variation of grain/cell size as a function of depth beneath the surface of fatigued GNG/CG Cu is plotted in Fig. 3f.

The foregoing experimental results elucidate two distinct mechanisms which synergistically influence fatigue characteristics in GNG/CG: (i) mechanically-driven grain coarsening in GNG layer,
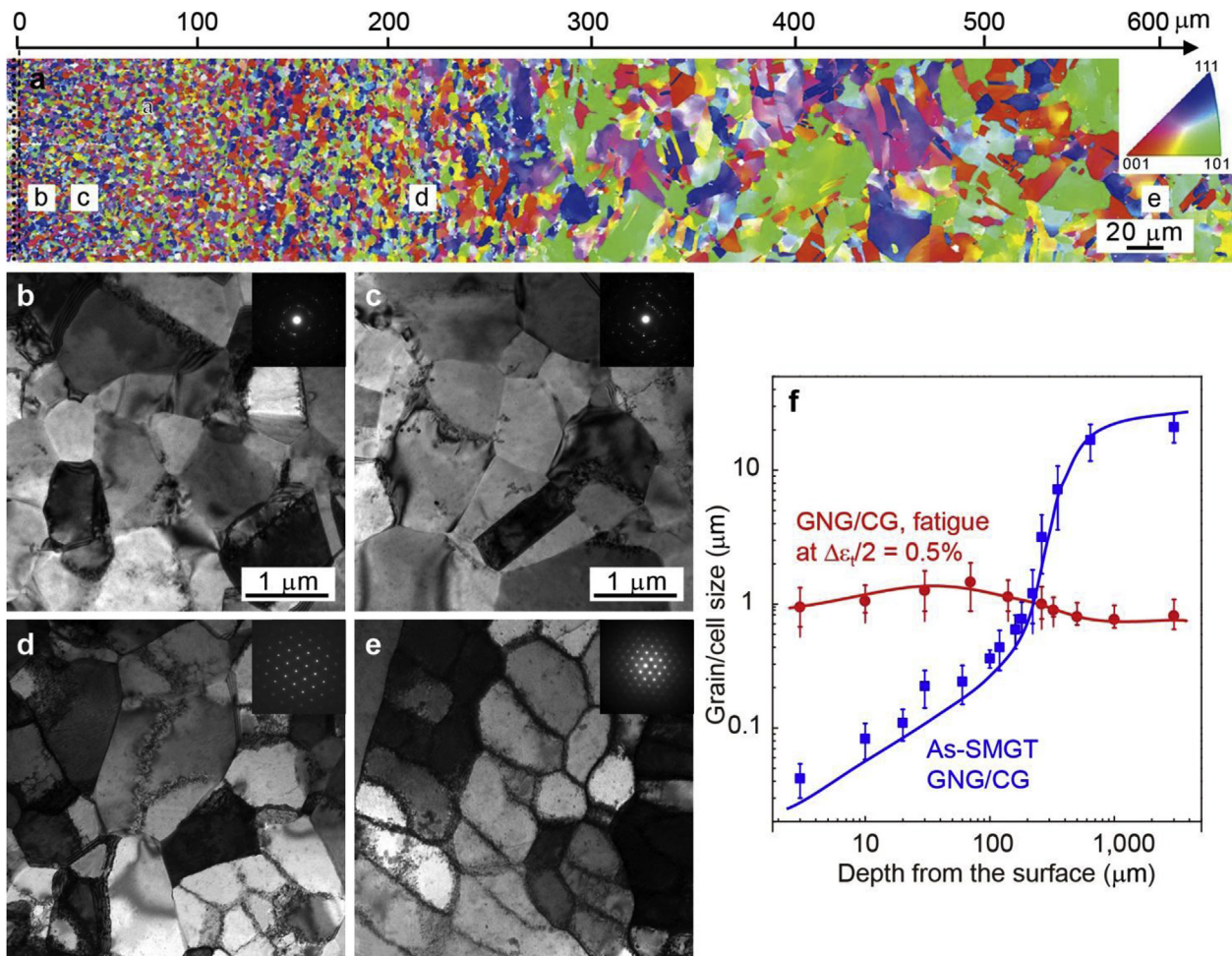


**Fig. 3. Fatigue-induced microstructure homogenization. a,** Cross-sectional EBSD image of GNG/CG Cu after repeated loading until failure over 2600 cycles at $\Delta\varepsilon_t/2$ of 0.5%. The bright-field TEM images corresponding to the regions marked "b", "c", "d" and "e" in Fig. 1a for the specimen prior to fatigue are shown here in **b-e**, respectively, after fatigue straining until failure. Top surface of the sample is indicated by a dashed line. Insets in **b-e** are SAED patterns. **f,** Variation of the average grain and/or cell size along the distance from the top surface to interior for GNG/CG Cu before and after cyclic failure at $\Delta\varepsilon_t/2$ of 0.5%.
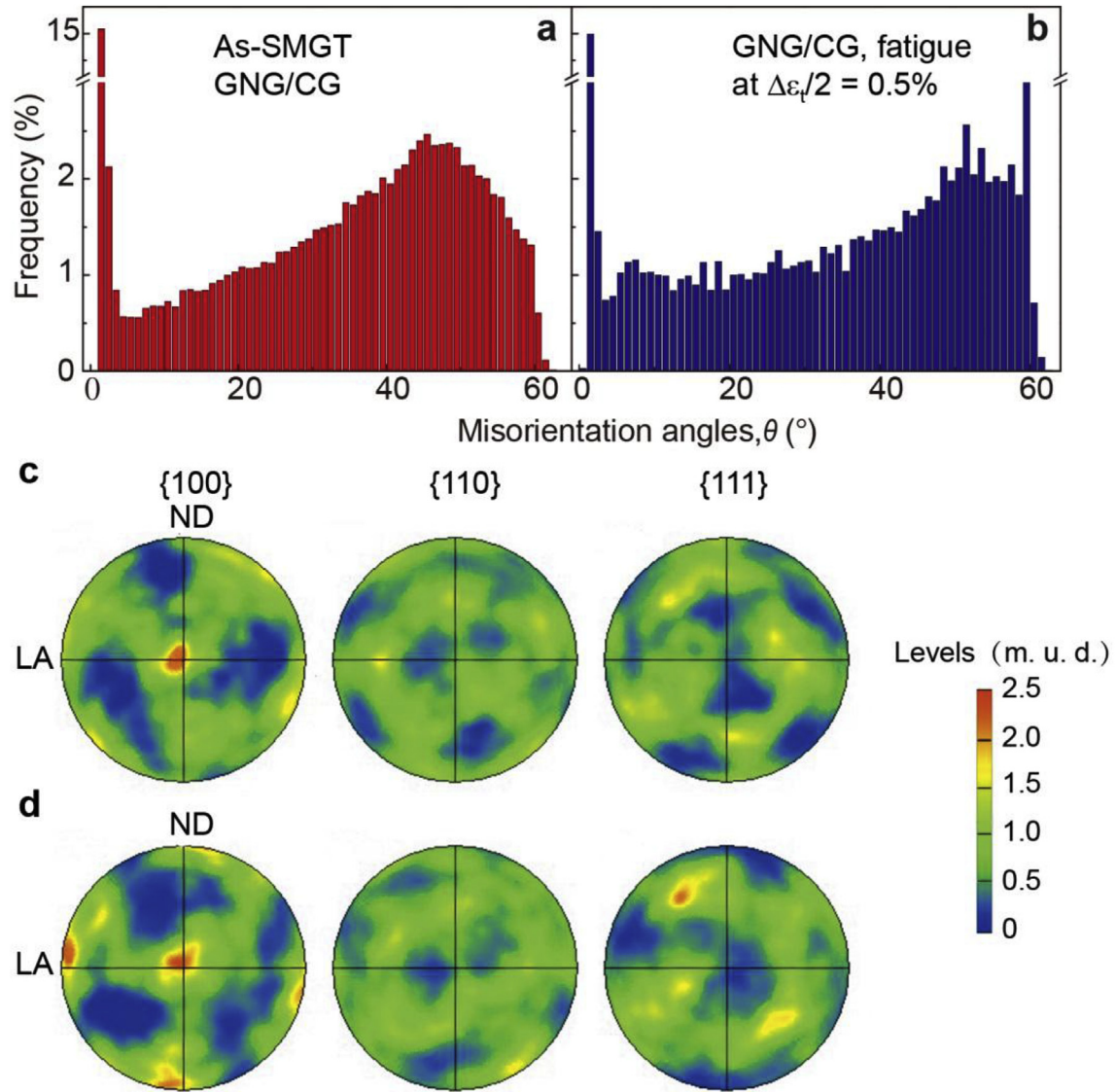
**Fig. 4.** The misorientation angle distributions (**a, b**) and Pole figures (**c, d**) of microstructures in the GNG layer of GNG/CG Cu (**a, c**) in the as-produced state (right after SMGT) and (**b, d**) after fatigue until failure at total strain amplitude ($\Delta\varepsilon_t/2$) of 0.5%.

and (ii) structural refinement in CG core arising from fatigue-induced dislocations that form intra-crystalline cells. Quantitative analysis of grain size and intra-crystalline cell size (Fig. 3f) reveals that the average size of both grains in GNG layer and dislocation cells in CG core converges to a common value of approximately 1 μm when a steady-state structure emerges upon cyclic loading. Fig. 3f further confirms that cyclic deformation induces homogenization of an initially heterogeneous structure from the top surface comprising nanograins (which coarsen) to the coarser-grained core (which is refined by fatigue-induced dislocation structures).

## 4. Discussion

### 4.1. Evolution of hardness and plastic strain during cycling loading

Fig. 6a is a plot of microhardness ($H_v$) versus depth from graded surface to core of GNG/CG samples after the first cycle, and after 4%, 40% and 100% of fatigue life cycles ($N_f$). Here $H_v$ decreases steeply with depth from the GNG layer (white background region) and remains essentially the same in CG core (blue background region)

in the specimen prior to the fatigue test. In the initial stages of fatigue cycle ($N < 4\%N_f$), cyclic hardening occurs in the CG core due to plastic deformation induced by high density dislocations (Figs. 5a and 6a). However, this leads to almost no changes in the microhardness of the GNG surface layer, because the GNG layer still deforms elastically with very limited microstructural recovery. Therefore, an obvious cyclic hardening detected in GNG/CG Cu in the early stage of fatigue life, as shown in Fig. 2c, is mainly contributed by the cyclic hardening of CG core.

With increasing cycles ($N > 4\%N_f$), coarsening of near-surface grains from cyclic straining (Fig. 3b and c) causes $H_v$ to decrease with increasing cycles, such that at $N = N_f$, hardness at 200 μm beneath the surface and becomes approximately same as that at surface, while the cyclic hardening in CG core becomes less pronounced. Collectively, this leads to a gradual loss of cyclic hardening of the whole GNG sample. These observations clearly demonstrate that the collective and integrated effects of cyclic hardening in the CG core and cyclic softening in the GNG layer lead to cyclic stability of GNG/CG samples. Note that dislocations in the CG core gradually rearrange to form cell structures and low-angle grain boundaries
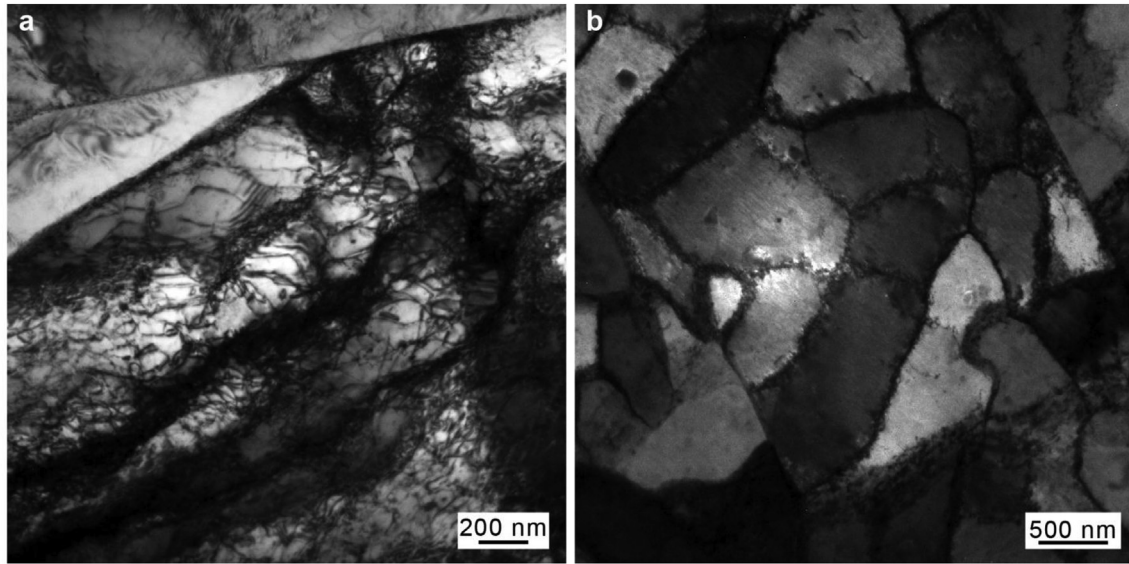
**Fig. 5.** TEM images of microstructures at CG core of GNG/CG Cu after different fatigue cycles ($N$) at $\Delta\varepsilon_t/2$ of 0.5%. (a) $N = 4\%N_f$, and (b) $N = N_f$, showing that dislocation cells are gradually formed during cyclic deformation.
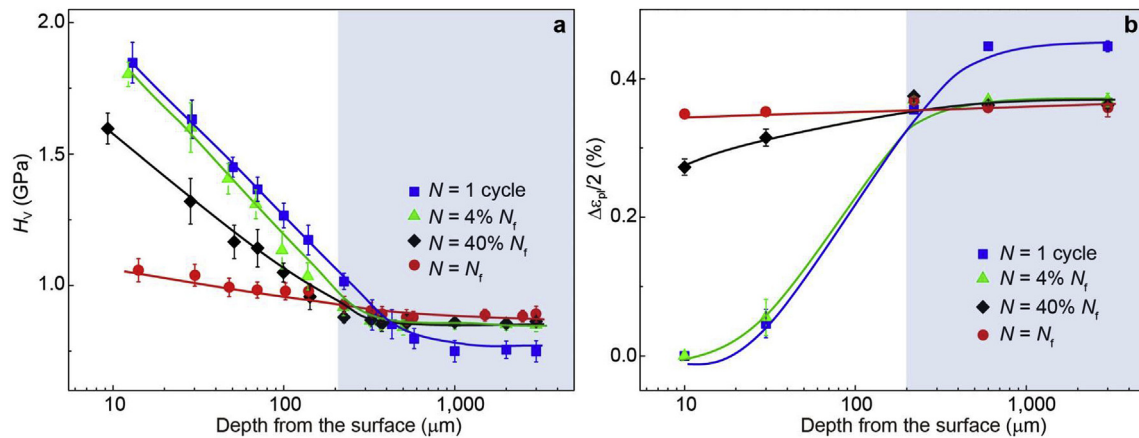


**Fig. 6.** Variations of hardness (**a**), plastic strain amplitude ($\Delta\varepsilon_{pl}/2$) (**b**) at different stages of fatigue failure life for GNG/CG Cu at $\Delta\varepsilon_t/2 = 0.5\%$. The area with the white background in **a** and **b** indicates top GNG surface layer while the area with the light blue background indicates the CG core. (For interpretation of the references to color in this figure legend, the reader is referred to the Web version of this article.)

(Fig. 3d, e and 5b). This "grain refinement" arising from cell formation leads to an average cell size that is comparable to the grain size of the coarsened near-surface grains of the GNG layer (Fig. 3f). The corresponding hardness values, $H_v$, of the two regions also become comparable (Fig. 6a).

The evolution of a stable grain size or cell size of about 1 μm in fatigued GNG/CG Cu is also consistent with estimates [1,2] for Cu that the critical distance necessary to activate transgranular dislocation loops to enhance dislocation density via the Frank-Reed mechanism, is of the order of 1 μm. Higher magnification images of micrographs such as Fig. 3e (and images similar to those shown in Fig. 5b) do indeed reveal the presence of such dislocation loops.

Given that the GNG/CG Cu specimens are cyclically deformed under fixed total strain amplitude, the plastic strain varies along the thickness of the graded structure which comprises gradations in grain size and strength. From measured $H_v$ data in Fig. 6a (see the detail in Appendix A), the plastic strain amplitude ($\Delta\varepsilon_{pl}/2$) distribution along depth for cyclically deformed GNG/CG Cu at different stages of fatigue is determined (Fig. 6b). As expected, the estimated

$\Delta\varepsilon_{pl}/2$ in CG core at 1st cycle is up to ~0.45%, the same as that of free-standing CG counterpart, while GNG layer deforms elastically, with no local plasticity, owing to its much higher strength. With increasing fatigue cycles, the hardening of CG core, and strain compatibility with the layers adjacent to the CG core cause progressively larger plastic deformation in the neighboring UFG layer. Finally, the NG layer at the surface begins to yield (Fig. 6b). At $N = N_f$, the plastic strain amplitude at the surface becomes comparable to that in CG core.

Our results also lead to the discovery that the graded surface nanostructure results in a plasticity gradient during fatigue straining through ordered, progressive plastic yielding and structural evolution across the thickness. While the graded NG and UFG surface layers become increasingly capable of accommodating plastic strain through grain coarsening (Fig. 3a–c) from fatigue, the CG core accommodates plasticity by the generation and rearrangement of dislocations into cell structures (Fig. 3d–e and Fig. 5). The attendant structural homogenization produces an accumulated plastic strain for the GNG/CG composite specimen which is

noticeably in excess of that achievable in the homogeneous CG or UFG specimens under similar strain conditions. (Note that a non-graded homogeneous NG Cu is not capable of sustaining fatigue deformation of the kind imposed on the present samples). This unprecedented result is plotted in Fig. 7 at a fixed cyclic strain amplitude of 0.5%, where the total accumulated plastic strain ($\sum 4\Delta\varepsilon_{\mathrm{pl}}/2$) in the GNG/CG specimen at failure is as large as $37.7 \pm 0.02$ and $23.4 \pm 0.09$ in the CG core and GNG surface layer, respectively. Remarkably, both these strain values are larger than the total plastic strain that can be accommodated during fatigue in homogeneous CG Cu: $20.2 \pm 1.1$ at $\Delta\varepsilon_t/2$ of 0.5%.

Initially soft microstructures (e.g., well-annealed homogeneous CG metals such as Cu) are known to cyclically harden [1,3,44] while initially hard microstructures (such as severely cold-worked metals) cyclically soften during fatigue [44,45]. This is ascribed to the fact that cyclic loading induces lattice defects/dislocation accumulation and formation or rearrangement of localized dislocation patterns in the former case [2–4], while the re-arrangement of pre-existing high density of dislocations occurs to reduce stored elastic energy in the latter case [1,44]. These two cases are known to reach a common steady-state structure upon fatigue loading, especially at very small-amplitude cyclic strain/stress, wherein the microstructure is populated with dislocation cells with a typical size of ~1 μm for pure metals, such as Cu [1,2,4]. This is similar to the final microstructure obtained in our present work for the GNG/CG Cu.

In homogeneous CG metals subjected to fatigue, accumulation of dislocations induced during cyclic straining and localization of deformation persistently along preferential intragranular planes facilitate plastic strain accommodation [1,2,6]. In the present case of GNG/CG Cu with graded structure, dislocation-assisted GB migration with concomitant grain coarsening (Fig. 3b and c) facilitates cyclic plastic deformation, as also seen in uniaxial tensile tests of these graded structures [35,46,47]. This process of GB migration is akin to an ordered GB migration that sweeps across the specimen without accumulating defects/dislocations in the present GNG/CG Cu, bearing resemblance to the cyclic deformation-induced defect healing in submicron-sized Al single crystals with higher density of pre-existing dislocations [48]. The orderly, progressive plasticity gradient with cyclic strain propagation from the soft CG core to the hard GNG surface during cyclic loading effectively suppresses the strain localization and helps to sustain an unusually large

accumulated cyclic plastic strain whose magnitude is even greater than 20 (i.e. 2000% strain) throughout the entire microstructure, as indicated in Fig. 7. Such large accumulated plastic strains have not been reported previously in homogeneous Cu subjected to the same fatigue conditions [1,11,15].

### 4.2. Strain delocalization and synergetic fatigue properties

SEM observations indicate that the surface of GNG/CG, even after repeated loading over 2600 cycles until failure at $\Delta\varepsilon_t/2$ of 0.5%, is "smooth" with only few damage features (Figs. 8b and 9a), compared to the control condition prior to fatigue testing (Fig. 8a). Confocal laser scanning microscopy (CLSM) observations in Fig. 8c show that the surface roughness of the GNG/Cu specimen is only 160 nm, which is an order of magnitude smaller than the large surface roughness (~1.7 μm) induced by mechanical fatigue in the homogeneous CG counterpart (Fig. 8e and f). Since fatigue-induced surface roughening is known to be a critical factor in the nucleation and subsequent propagation of fatigue cracks [1,7], the smooth surfaces of the fatigued GNG/Cu structure are far less susceptible to formation of microcracks (Fig. 8b and c). The cross-sectional SEM image of GNG layer after failure shows that the micro-cracks nucleate from the outermost surface, as highlighted by the blue arrows in Fig. 9b. By contrast, numerous microcracks resulted from surface extrusions/intrusions in the homogeneous CG Cu subjected to fatigue (Fig. 8e and f). In fatigued CG metals, typical cyclic-straining-induced microstructures such as deformation bands, persistent slip bands or cell structures, lead to large surface roughening [2,24]. Such surface roughening and the resultant fatigue damage and failure are effectively suppressed in the GNG layer because that their characteristic structural dimensions are much greater than or at least comparable to the grain size in the GNG structure.

Suppression of strain localization during cyclic deformation, therefore, rationalizes enhancement in low-cycle fatigue life of CG Cu with a GNG surface layer, compared to that of the homogeneous CG counterpart. At the same time, a much greater fatigue endurance limit under stress-controlled cyclic deformation (so-called high-cycle fatigue), arises from the presence of surface GNG structure, which not only contributes to the high fatigue strength but also suppresses strain localization and increases the resistance to fatigue crack initiation [49].

Fig. 10 shows this remarkable dual benefit of this graded surface nanostructure for the present GNG/CG Cu. It is a plot of the fatigue endurance limit (which represents the resistance of the specimen to low-amplitude, high-cycle fatigue) as a function of the transition life (see the detail in Appendix B), which signifies the level of resistance to both short-life (plasticity-dominated) and long-life (primarily nominal elasticity dominated) fatigue. Specifically, the transition life is defined as the total number of fatigue reversals that the material is capable of sustaining at the intersection of low-cycle (large-strain) and high-cycle (small-strain) fatigue lives, i.e. at a $\Delta\varepsilon_t/2$ with the elastic and plastic strain components of total fatigue life intersected (see Supplementary Fig. 1). Also shown for comparison are data for pure Cu with homogeneous CG and UFG structures, and for bimodal structures comprising CG and UFG [11,14,16,17,21,50–55]. A trade-off between the transition life and fatigue limit is generally seen for face-centered cubic metals with homogenous microstructure [8,11,12] and bimodal microstructures with CG randomly distributed in UFG matrix [11,15]. The transition life for homogeneous Cu usually drops dramatically with decreasing grain size, especially when the fatigue limit is above 75 MPa. However, the present graded surface nanostructure provides a superior fatigue resistance of GNG/CG Cu in both low-cycle and high cycle regimes: with the transition life nearly comparable
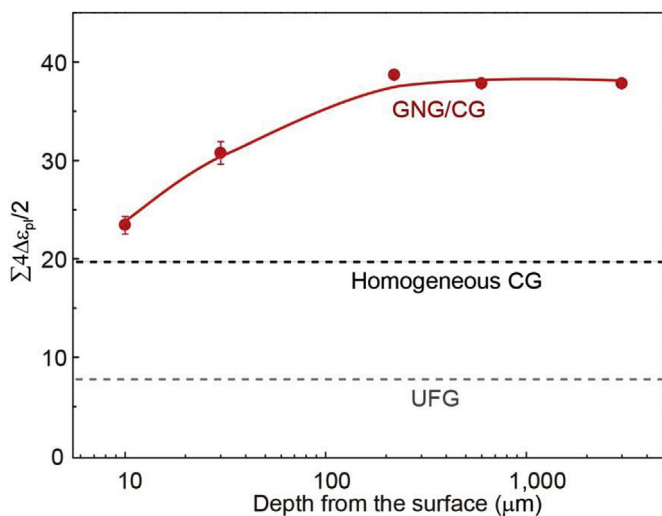


**Fig. 7.** The accumulated plastic strain ($\sum 4\Delta\varepsilon_{\mathrm{pl}}/2$) as a function of depth from the top surface for GNG/CG, homogeneous CG and UFG Cu fatigued to failure at $\Delta\varepsilon_t/2 = 0.5\%$.
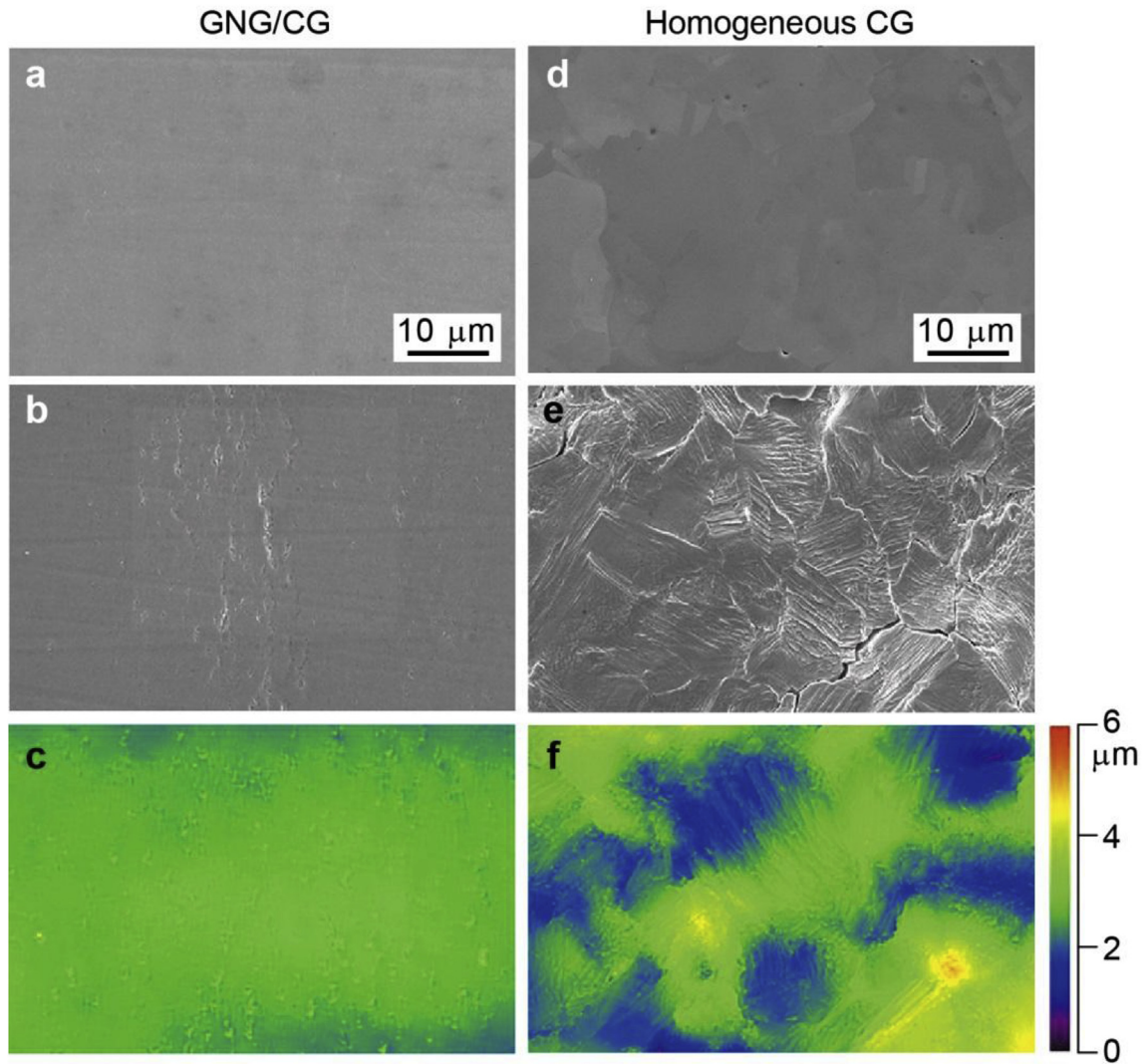
**Fig. 8.** Surface morphologies of GNG/CG Cu before (a, SEM) and after failure at $\Delta\varepsilon_t/2$ of 0.5% (b, SEM and c, CLSM 3D profiles). For comparison, the surface morphology of homogeneous CG before (d) and after cyclic deformation at the same $\Delta\varepsilon_t/2$ (e and f) are included. The contrast in c and f indicates the height variation in surface roughness morphology measured by the color bar on the right.
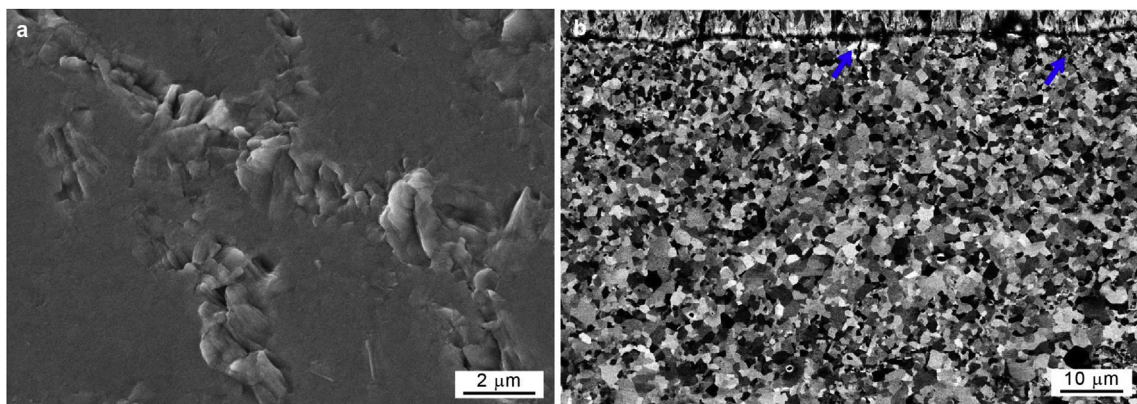


**Fig. 9.** Side surface view (**a**) and Cross-sectional (**b**) SEM images of GNG/CG Cu after failure at $\Delta\varepsilon_t/2$ of 0.5%, showing fatigue cracks are formed at the sample surface, owing to cyclic deformation induced surface roughening.
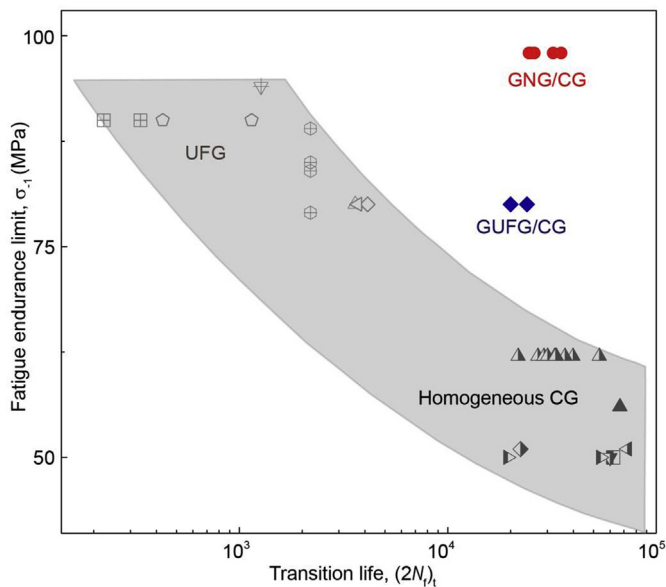
**Fig. 10.** Synergetic fatigue properties of gradient nanostructure. Correlation between the fatigue endurance limit ($\sigma_{-1}$) and the transition life ($(2N_f)_t$) of GNG/CG and GUFG/CG Cu. Literature data for homogeneous CG Cu and UFG Cu are also shown.

to that of CG Cu, together with a significantly higher fatigue limit of ~100 MPa which is nearly twice that of CG Cu (Fig. 10).

### 4.3. Thin nanograin surface layer effect on fatigue resistance

In order to further investigate and isolate the effect of the thin NG surface layer on fatigue resistance, we conducted another set of experiments where the 20 μm-thick surface NG layer was removed from the specimen, exposing only the UFG layer at the top surface. This specimen is hereafter referred to as graded ultra-fine grained (GUFG/CG) Cu. Both fatigue limit and transition life of GUFG/CG Cu are lower than those of GNG/NG Cu, as seen from Fig. 2a and b and 9. GUFG/Cu shows numerous fatigue microcracks at final failure, although its final surface roughness is comparable (~190 nm) to that of GNG/CG Cu. Besides, the cyclic stress for GUFG/CG Cu is slightly lower than that of GNG/CG counterparts fatigued at the same strain amplitude (Fig. 2b). This suggests that the NG surface layer, albeit only accounting for very small fraction (~1.3%) of the entire fatigue specimen, plays a more critical role in enabling high fatigue limit and fatigue life, than the UFG layer.

The SGMT process used to produce the GNG surface on the CG Cu core also induces compressive residual stresses at the top surface. Somewhat analogous to the shot-peening process [1], the layer of compressive residual stress is expected to have a mild beneficial effect in the very early cycles of loading. Its effect on the overall fatigue response of GNG metals during low cycle fatigue seen here is minimal given that the GNG layer constitutes only a small fraction of the overall volume of the specimen. Furthermore, with continuous microstructural evolution in response to fatigue loading, any effect of the residual stress on the overall fatigue behavior is expected to vanish after a few initial cycles because of significant grain growth and the overall homogenization of grain structure throughout the specimen [41,56].

## 5. Conclusion

Our study demonstrates that "coating" CG with a thin graded nanostructure skin can thus produce an unprecedented combination of cyclic properties: doubling both low-cycle fatigue life and high-cycle fatigue limit, compared to its homogenous CG counterparts. Such superior fatigue resistance stems from an ordered strain accommodation and delocalization process with significantly reduced intragranular dislocation accumulation, i.e. the progressive homogenization of an initially graded heterogeneous microstructure through ordered cyclic plastic strain transmission from CG core to GNG surface layer and effective suppression of surface roughening. Our method for preparing GNG samples with superior fatigue properties is scalable for any size and shape and is amenable to a wide variety of processing methods to create surface nanostructures. Furthermore, the mechanisms underlying the beneficial effects of grading the surface layer in enhancing fatigue resistance are general and broadly applicable to a wide variety of engineering alloys used in major structural applications. Therefore, the findings of this work and the flexibility they offer in tailoring the geometry, grain size and gradation of the surface layer to enhance both high-cycle and low-cycle fatigue resistance offer novel opportunities in material design to improve the performance of engineering components of practical interest.

## Appendix A. Supplementary data

Supplementary data to this article can be found online at https://doi.org/10.1016/j.actamat.2018.12.018.

## References

[1] S. Suresh, Fatigue of Materials, second ed., Cambridge University Press, Cambridge, 1998.
[2] P. Peralta, C. Laird, Fatigue of metals, in: D.E. Laughlin, K. Hono (Eds.), Physical Metallurgy, fifth ed., Elsevier, Oxford, 2014, pp. 1765—1880.
[3] P. Lukáš, M. Klesnil, Cyclic stress-strain response and fatigued life of metals in low amplitude region, Mater. Sci. Eng. 11 (1973) 345—356.
[4] H. Mughrabi, Dislocation wall and cell structures and long-range internal stresses in deformed metal crystals, Acta Metall. 31 (1983) 1367—1379.
[5] Z.S. Basinski, S.J. Basinski, Fundamental aspects of low amplitude cyclic deformation in face-centred cubic crystals, Prog. Mater. Sci. 36 (1992) 89—148.
[6] P.J.E. Forsyth, Exudation of material from slip bands at the surface of fatigued crystals of an aluminium copper alloy, Nature 171 (1953) 172—173.
[7] N. Thompson, N. Wadsworth, N. Louat, The origin of fatigue fracture in copper, Philos. Mag. A 1 (1956) 113—126.
[8] M.A. Meyers, A. Mishra, D.J. Benson, Mechanical properties of nanocrystalline materials, Prog. Mater. Sci. 51 (2006) 427—556.
[9] T. Hanlon, Y.N. Kwon, S. Suresh, Grain size effects on the fatigue response of nanocrystalline metals, Scripta Mater. 49 (2003) 675—680.
[10] T. Hanlon, E.D. Tabachnikova, S. Suresh, Fatigue behavior of nanocrystalline metals and alloys, Int. J. Fatig. 27 (2005) 1147—1158.
[11] H. Mughrabi, H.W. Höppel, Cyclic deformation and fatigue properties of very fine-grained metals and alloys, Int. J. Fatig. 32 (2010) 1413—1427.
[12] A. Pineau, A. Amine Benzerga, T. Pardoen, Failure of metals III: fracture and fatigue of nanostructured metallic materials, Acta Mater. 107 (2016) 508—544.
[13] C.C. Koch, D.G. Morris, K. Lu, A. Inoue, Ductility of nanostructured materials, MRS Bull. 24 (1999) 54—58.
[14] S.R. Agnew, A.Y. Vinogradov, S. Hashimoto, J.R. Weertman, Overview of fatigue performance of Cu processed by severe plastic deformation, J. Electron. Mater. 28 (1999) 1038—1044.
[15] H.W. Höppel, M. Brunnbauer, H. Mughrabi, Cyclic deformation behaviour of utrafine-grained size copper produced by equal channel angular pressing, in: Werkstoffwoche-Partnerschaft (Ed.), Proceedings of Materials Week 2000, Frankfurt, German, 2000, pp. 1—8.
[16] A. Vinogradov, S. Hashimoto, Multiscale phenomena in fatigue of ultra-fine grain materials - an overview, Mater. Trans., JIM 42 (2001) 74—84.
[17] P. Lukáš, L. Kunz, M. Svoboda, Fatigue mechanisms in ultrafine-grained copper, Kovove Mater. 47 (2009) 1—9.
[18] K. Lu, L. Lu, S. Suresh, Strengthening materials by engineering coherent

internal boundaries at the nanoscale, Science 324 (2009) 349—352.

[19] A. Singh, L. Tang, M. Dao, L. Lu, S. Suresh, Fracture toughness and fatigue crack growth characteristics of nanotwinned copper, Acta Mater. 59 (2011) 2437—2446.

[20] C.J. Shute, B.D. Myers, S. Xie, S.Y. Li, T.W. Barbee Jr., A.M. Hodge, J.R. Weertman, Detwinning, damage and crack initiation during cyclic loading of Cu samples containing aligned nanotwins, Acta Mater. 59 (2011) 4569—4577.

[21] Q.S. Pan, L. Lu, Strain-controlled cyclic stability and properties of Cu with highly oriented nanoscale twins, Acta Mater. 81 (2014) 248—257.

[22] Q.S. Pan, H.F. Zhou, Q.H. Lu, H.J. Gao, L. Lu, History-independent cyclic response of nanotwinned metals, Nature 551 (2017) 214—217.

[23] L.L. Zhu, H.H. Ruan, X.Y. Li, M. Dao, H.J. Gao, J. Lu, Modeling grain size dependent optimal twin spacing for achieving ultimate high strength and related high ductility in nanotwinned metals, Acta Mater. 59 (2011) 5544—5557.

[24] S. Suresh, Graded materials for resistance to contact deformation and damage, Science 292 (2001) 2447—2451.

[25] I.S. Choi, A.J. Detor, R. Schwaiger, M. Dao, C.A. Schuh, S. Suresh, Mechanics of indentation of plastically graded materials - II: experiments on nanocrystal-line alloys with grain size gradients, J. Mech. Phys. Solid. 56 (2008) 172—183.

[26] S. Suresh, A. Mortensen, Fundamentals of Functionally Graded Materials, The Institute of Materials, London, UK, 1998.

[27] J. Jitcharoen, N.P. Padture, A.E. Giannakopoulos, S. Suresh, Hertzian-crack suppression in ceramics with elastic-modulus-graded surfaces, J. Am. Chem. Soc. 81 (1998) 2301—2308.

[28] D.C. Pender, N.P. Padture, A.E. Giannakopoulos, S. Suresh, Gradients in elastic modulus for improved contact-damage resistance. Part I: the silicon nitride-oxynitride glass system, Acta Mater. 49 (2001) 3255—3262.

[29] S. Suresh, M. Olsson, A.E. Giannakopoulos, N.P. Padture, J. Jitcharoen, Engi-neering the resistance to sliding-contact damage through controlled gradients in elastic properties at contact surfaces, Acta Mater. 47 (1999) 3915—3926.

[30] S.B. Yi, T. Ludian, L. Wagner, Investigation of deformation gradients in surface zone of mechanically surface treated CuZn30, Mater. Sci. Forum 561—565 (2007) 2229—2232.

[31] R.K. Nalla, I. Altenberger, U. Noster, G.Y. Liu, B. Scholtes, R.O. Ritchie, On the influence of mechanical surface treatments - deep rolling and laser shock peening - on the fatigue behavior of Ti-6Al-4V at ambient and elevated temperatures, Mater. Sci. Eng., A 355 (2003) 216—230.

[32] K. Lu, J. Lu, Nanostructured surface layer on metallic materials induced by surface mechanical attrition treatment, Mater. Sci. Eng. A 375 (2004) 38—45.

[33] S.Q. Deng, A. Godfrey, W. Liu, N. Hansen, A gradient nanostructure generated in pure copper by platen friction sliding deformation, Scripta Mater. 117 (2016) 41—45.

[34] X.H. Zhao, Y.J. Zhang, Y. Liu, Surface characteristics and fatigue behavior of gradient nano-structured magnesium alloy, Metals 7 (2017) 62.

[35] T.H. Fang, W.L. Li, N.R. Tao, K. Lu, Revealing extraordinary intrinsic tensile plasticity in gradient nano-grained copper, Science 331 (2011) 1587—1590.

[36] X.L. Wu, P. Jiang, L. Chen, F.P. Yuan, Y.T.T. Zhu, Extraordinary strain hardening by gradient structure, Proc. Natl. Acad. Sci. U.S.A. 111 (2014) 7197—7201.

[37] Y.J. Wei, Y.Q. Li, L.C. Zhu, Y. Liu, X.Q. Lei, G. Wang, Y.X. Wu, Z.L. Mi, J.B. Liu, H.T. Wang, H.J. Gao, Evading the strength-ductility trade-off dilemma in steel

through gradient hierarchical nanotwins, Nat. Commun. 5 (2014) 3580.

[38] H.N. Kou, J. Lu, Y. Li, High-strength and high-ductility nanostructured and amorphous metallic materials, Adv. Mater. 26 (2014) 5518—5524.

[39] T. Roland, D. Retraint, K. Lu, J. Lu, Fatigue life improvement through surface nanostructuring of stainless steel by means of surface mechanical attrition treatment, Scripta Mater. 54 (2006) 1949—1954.

[40] J.W. Tian, J.C. Villegas, W. Yuan, D. Fielden, L. Shaw, P.K. Liaw, D.L. Klarstrom, A study of the effect of nanostructured surface layers on the fatigue behaviors of a C-2000 superalloy, Mater. Sci. Eng., A 468 (2007) 164—170.

[41] J.Z. Long, Q.S. Pan, N.R. Tao, L. Lu, Residual stress induced tension-compression asymmetry of gradient nanograined copper, Mater. Res. Lett. 6 (2018) 456—461.

[42] L. Kunz, P. Lukáš, M. Svoboda, Fatigue strength, microstructural stability and strain localization in ultrafine-grained copper, Mater. Sci. Eng., A 424 (2006) 97—104.

[43] P. Xue, Z.Y. Huang, B.B. Wang, Y.Z. Tian, W. Wang, B.L. Xiao, Z.L. Ma, Intrinsic high cycle fatigue behavior of ultrafine grained pure Cu with stable structure, Sci. China. Mater. 59 (2016) 1—7.

[44] C.E. Feltner, C. Laird, Cyclic stress-strain response of FCC metals and alloys 1. phenomenological experiments, Acta Metall. 15 (1967) 1621—1632.

[45] N.H. Polakowski, Softening of cold-worked metals under cyclic strains, Nature 171 (1953), 173-173.

[46] W. Chen, Z.S. You, N.R. Tao, Z.H. Jin, L. Lu, Mechanically-induced grain coarsening in gradient nano-grained copper, Acta Mater. 125 (2017) 255—264.

[47] K. Zhang, J.R. Weertman, J.A. Eastman, The influence of time, temperature, and grain size on indentation creep in high-purity nanocrystalline and ultrafine grain copper, Appl. Phys. Lett. 85 (2004) 5197—5199.

[48] Z.J. Wang, Q.J. Li, Y.N. Cui, Z.L. Liu, E. Ma, J. Li, J. Sun, Z. Zhuang, M. Dao, Z.W. Shan, S. Suresh, Cyclic deformation leads to defect healing and strengthening of small-volume metal crystals, Proc. Natl. Acad. Sci. U.S.A. 112 (2015) 13502—13507.

[49] L. Yang, N.R. Tao, K. Lu, L. Lu, Enhanced fatigue resistance of Cu with a gradient nanograined surface layer, Scripta Mater. 68 (2013) 801—804.

[50] J. Polák, M. Klesnil, Cyclic stress-strain response and dislocation structures in polycrystalline copper, Mater. Sci. Eng. 63 (1984) 189—196.

[51] P. Lukáš, L. Kunz, Effect of grain-size on the high cycle fatigue behavior of polycrystalline copper, Mater. Sci. Eng. 85 (1987) 67—75.

[52] M. Korn, R. Lapovok, A. Bohner, H.W. Höppel, H. Mughrabi, Bimodal grain size distributions in UFG materials produced by SPD - their evolution and effect on the fatigue and monotonic strength properties, Kovove Mater. 49 (2011) 51—63.

[53] A.W. Thompson, W.A. Backofen, Effect of grain size on fatigue, Acta Metall. 19 (1971) 597—606.

[54] X.H. An, S.D. Wu, Z.G. Wang, Z.F. Zhang, Enhanced cyclic deformation re-sponses of ultrafine-grained Cu and nanocrystalline Cu—Al alloys, Acta Mater. 74 (2014) 200—214.

[55] H.Z. Ding, H. Mughrabi, H.W. Höppel, A low-cycle fatigue life prediction model of ultrafine-grained metals, Fatig. Fract. Eng. Mater. 25 (2002) 975—984.

[56] H.W. Huang, Z.B. Wang, J. Lu, K. Lu, Fatigue behaviors of AISI 316L stainless steel with a gradient nanostructured surface layer, Acta Mater. 87 (2015) 150—160.